Dynamic Regulation of Endothelial Nitric Oxide Synthase: Complementary Roles of Dual Acylation and Caveolin Interactions†

Olivier Feron, Jeffrey B. Michel, Kazuhiro Sase, and Thomas Michel*

Cardiovascular Division, Department of Medicine, Brigham and Women's Hospital, Harvard Medical School, 75 Francis Street, Boston, Massachusetts 02115

Received September 16, 1997; Revised Manuscript Received October 29, 1997⊗

ABSTRACT: N-Terminal myristoylation and thiopalmitoylation of the endothelial isoform of nitric oxide synthase (eNOS) are required for targeting the enzyme to specialized signal-transducing microdomains of plasma membrane termed caveolae. We have previously documented that the subcellular localization of eNOS is dynamically regulated by agonists such as bradykinin, which promotes enzyme depalmitoylation and translocation from caveolae. More recently, we have shown that association of eNOS with caveolin, the principal structural protein in caveolae, leads to enzyme inhibition, in a reversible process modulated by Ca^{2+}−calmodulin (CaM). We now report studies of the respective roles of acylation and caveolin interaction for regulating eNOS activity. Using eNOS truncation and deletion mutants expressed in COS-7 cells, we have identified an obligatory role for the N-terminal half of eNOS in stabilizing its association with caveolin. By exploring the differential effects of detergents (CHAPS *vs* octyl glucoside), we have shown that this direct interaction between both proteins is facilitated by, but does not require, eNOS acylation, and, importantly, that treatment of intact aortic endothelial cells with the calcium ionophore A23187 leads to the rapid disruption of the eNOS−caveolin complexes. Finally, using transiently transfected COS-7 cells, we have observed that the myristoylation-deficient cytosol-restricted eNOS mutant (myr^-) as well as the cytosolic fraction of the palmitoylation-deficient eNOS mutant ($palm^-$) may both interact with caveolin; this association also leads to a marked inhibition of enzyme activity, which is completely reversed by addition of calmodulin. We conclude that the regulatory eNOS−caveolin association is independent of the state of eNOS acylation, indicating that agonist-evoked Ca^{2+}/CaM-dependent disruption of the caveolin−eNOS complex, rather than agonist-promoted depalmitoylation of eNOS, relieves caveolin's tonic inhibition of enzyme activity. We therefore propose that caveolin may serve as an eNOS chaperone regulating NO production independently of the enzyme's residence within caveolae or its state of acylation.

Nitric oxide (NO)[1] is an important signaling molecule involved in many biological processes, and is synthesized in mammalian cells by a family of calmodulin-activated NO synthases (NOS) (*1*−*3*). The endothelial NOS (eNOS) is unique among the NOS isoforms in its being dually acylated by the fatty acids myristate and palmitate (*4*−*6*). While myristoylation is an essentially irreversible protein modification occurring cotranslationally on N-terminal glycine residues within a specific consensus sequence (*7*), thiopalmitoylation is a reversible post-translational modification for which no unique consensus sequence exists (*8*). The myristoylation-deficient eNOS mutant (myr^-, which is neither myristoylated nor palmitoylated, is almost entirely localized in the cytosol (*4*, *6*). We have previously reported that both myristoylation and palmitoylation are required to target eNOS to specialized plasmalemmal microdomains named caveolae, each acylation process enhancing the caveolar enrichment by 10-fold (*9*). Caveolae are plasma membrane invaginations enriched in cholesterol and various signaling molecules including receptors, transducer, and effector proteins (*10*−*12*). Lipid modification, including prenylation as well as acylation, is a common feature for many of the signaling proteins targeted to caveolae, such as members of the Src family of protein tyrosine kinases (PTK) (*13*) as well as heterotrimeric and small G-proteins (*14*, *15*) and caveolin itself, the structural "coat" protein of caveolae (*16*, *17*).

† This work was supported by awards (to T.M.) from the National Institutes of Health (Grant HL46457), the American Heart Association, and the Burroughs Wellcome Fund. O.F. is a Senior Research Assistant of the National Fund for Scientific Research (FNRS, Belgium). J.B.M. is a Bugher−American Heart Association Fellow in Cardiovascular Molecular Biology. T.M. is an Established Investigator of the American Heart Association and a Burroughs Wellcome Scholar in Experimental Therapeutics.

* To whom correspondence should be addressed at Cardiovascular Division, Brigham and Women's Hospital, Harvard Medical School, Thorn Building 1110A, 75 Francis St., Boston, MA 02115. E-mail: michel@calvin.bwh.harvard.edu. Phone: 617-732-7376. Fax: 617-732-5132.

⊗ Abstract published in *Advance ACS Abstracts,* December 15, 1997.

[1] Abbreviations: NO, nitric oxide; NOS, nitric oxide synthase; eNOS, endothelial isoform of NOS; CaM, calmodulin; $palm^-$, palmitoylation-deficient eNOS mutant; myr^-, myristoylation-deficient eNOS mutant; WT, wild-type; BAEC, bovine aortic endothelial cells; CHAPS, 3-[(3-cholamidopropyl)dimethylammonio]-1-propanesulfonic acid; OG, octyl glucoside; GPI, glycosylphosphatidylinositol; PTK, protein tyrosine kinase.

S0006-2960(97)02307-6 CCC: $15.00
Published on Web 01/06/1998

The role and regulation of protein lipidation in the targeting of signaling proteins to plasmalemmal caveolae are incompletely understood. Mutagenesis studies have documented that myristoylation of G-protein α subunits (*18*) or palmitoylation of caveolin (*16*) is not required for their caveolar localization, whereas thiopalmitoylation of PTK (*13*) and prenylation of H-Ras (*19*) are both necessary and sufficient to confer localization of these proteins to caveolae. Moreover, since palmitoylation may undergo dynamic regulation by agonists (for refs, see *8* and *15*), this specific acylation may play a critical role in the reversible caveolar targeting of signaling proteins, and in the modulation of their biologic activity. For example, we have reported that bradykinin promotes eNOS depalmitoylation (*20*), and thereby could importantly influence the agonist response by promoting enzyme translocation from plasmalemmal caveolae to other cell compartments. The agonist-induced translocation of eNOS from caveolae likely leads to local changes in cofactor and substrate availability for the enzyme, and may also modulate the interaction of eNOS with other caveolae-targeted signaling proteins, with important consequences for the cellular regulation of NO synthesis.

Several recent reports have presented evidence for direct regulatory interactions between caveolin and diverse lipid-modified signaling proteins including PTK, G-protein α subunits, and H-Ras (*21*, *22*), perhaps indicating that protein−protein interactions may influence the caveolar targeting of signaling molecules. In similar fashion, we have shown that eNOS can be quantitatively immunoprecipitated by antibodies directed against caveolin (*23*). In addition, we have recently found that the interaction of eNOS with caveolin leads to a profound inhibition of eNOS enzyme activity, and that Ca^{2+}−calmodulin relieves the inhibition of eNOS by caveolin (*24*). These studies raise important questions regarding the cellular regulation of eNOS−caveolin interactions in the context of enzyme acylation. Does eNOS need to be targeted (by acylation) to caveolae in order to interact with caveolin? Alternatively, is it the interaction of caveolin with eNOS that is responsible for targeting the enzyme to caveolae where palmitoylation may then occur? Is eNOS depalmitoylation required for its dissociation from caveolin (and subsequent enzyme activation)? Alternatively, does caveolin remain associated (or reassociate) with eNOS following the latter's depalmitoylation and translocation to noncaveolar subcellular compartments? The present studies explore the interactions between caveolin and various eNOS acylation and deletion mutants in transfected COS-7 cells, and investigate the regulation of eNOS−caveolin interactions in intact endothelial cells.

EXPERIMENTAL PROCEDURES

Plasmid Constructs. cDNA constructs encoding wild-type eNOS, the myristoylation-deficient mutant (myr^-), or the palmitoylation-deficient mutant ($palm^-$) have previously been described (*4*, *6*, *19*). The myristoylation-deficient mutant eNOS (glycine at position 2 changed to alanine) and the palmitoylation-deficient mutant eNOS (cysteine residues at positions 15 and 26 changed to serine) were generated by PCR-based mutagenesis using the wild-type eNOS cDNA as template, and have been previously characterized (*4*, *6*). Truncation and deletion mutants have also been described and characterized previously (*19*, *25*). Briefly, truncation mutants of bovine eNOS lacking either the N-terminal (Δ1−511) or the C-terminal (Δ528−1205) domains have been created using propitious restriction enzyme sites within the eNOS cDNA sequence, a *Bgl*II site (at bp 1536) and a *Bsa*I site (at bp 1598), respectively. Deletion mutants lacking aa 13−506 (Δ12−507) and aa 86−506 (Δ85−507) were created by removing the sequence in the eNOS cDNA between the *Ava*I site (at bp 50) and the *Bgl*II site (at bp 1536), and between the *Dra*III site (at bp 273) and the *Bgl*II site (at bp 1536), respectively. These different constructs have all been subcloned into pK-CMV expression vector, as previously described (*19*). Caveolin-1 cDNA in the eukaryotic expression vector pCB-7 was obtained from Michael Lisanti (Whitehead Institute, Cambridge).

Cell Cultures and Cell Transfection. COS-7 cells and bovine aortic endothelial cells (BAEC) were cultured as described (*4*, *6*, *23*). COS-7 cells were transfected with the plasmid cDNA in 100-mm cell culture plates using Lipofectamine (Life Technologies, Gaithersburg, MD) according to the manufacturer's protocol; an irrelevant plasmid encoding β-galactosidase was used as a control to maintain identical amounts of DNA in each transfection.

Preparation of Cellular Lysates and Subcellular Fractionation. Transfected COS-7 cells or BAEC were harvested by scraping in phosphate-buffered saline, pelleted by centrifugation, and then resuspended in a "CHAPS buffer", containing 50 mM Tris-HCl (pH 7.4), 20 mM CHAPS, 125 mM NaCl, 2 mM dithiothreitol, 0.1 mM EGTA, and protease inhibitors (1 mg/mL leupeptin, 1 mg/mL pepstatin, and 1 mM phenymethanesulfonyl fluoride), as previously described (*23*−*25*). In some experiments, the 20 mM CHAPS detergent was replaced by 60 mM octyl glucoside (OG). Cells were lysed by sonication (three 10-s bursts, output power 1) using a Branson sonifier 450 (Branson Ultrasonic Corp., Danbury, CT); cell debris was discarded following a brief 1000*g* centrifugation. When cell fractionation was required, cells were first lysed by sonication in a hypotonic buffer and separated into soluble and particulate fractions by ultracentrifugation (100000*g*, 1 h), as previously described (*4*, *6*, *19*, *25*).

Immunoprecipitation. Aliquots of cell lysates were incubated with rabbit anti-caveolin-1 or anti-eNOS polyclonal antibodies (Transduction Labs) at a final concentration of 4 μg/mL; antibody titration experiments (not shown) documented that this concentration led to quantitative immunoprecipitation of caveolin from cell lysates. The isoform specificity and lack of cross-reactivity of these antibodies have been previously established (*23*). After 1 h at 4 °C, protein G−Sepharose beads (50 mL of a 50% slurry) were added to the supernatant for a further 1-h incubation at 4 °C. Bound immune complexes were washed 3 times with CHAPS or OG buffer and then once with 50 mM Tris-HCl (pH 7.4), 150 mM NaCl. Immunoprecipitated proteins were then eluted by boiling for 5 min in Laemmli sample buffer.

SDS−PAGE and Immunoblotting. Denatured immunoprecipitated proteins were loaded and separated on 7.5 or 12% SDS−polyacrylamide gels and transferred to a PVDF membrane (BioRad). After blocking with 5% non-fat dry milk in Tris-buffered saline with 0.1% (v/v) Tween 20 (TBST; Sigma), membranes were incubated with primary antibodies directed against the C-terminal (Transduction Labs) or N-terminal end (Santa Cruz) of eNOS, or against

caveolin-1 (Transduction Labs) for 1 h in TBST containing 1% non-fat dry milk. After 4 washes (15 min each), the membranes were incubated for 1 h with a horseradish peroxidase-conjugated secondary antibody (Jackson ImmunoResearch Labs) at a 1:10 000 dilution in TBST containing 1% non-fat dry milk. After 4 additional washes in TBST, the membranes were rinsed once in TBST, incubated with a chemiluminescent reagent according to the manufacturer's protocols (Renaissance, DuPont NEN), and exposed to X-ray film.

Nitric Oxide Synthase Activity. NOS activity was determined in transfected COS-7 cell lysates or subcellular fractions by measuring the conversion of [^{3}H]arginine to [^{3}H]-citrulline, as previously described (26).

RESULTS

Interaction of Truncation and Deletion eNOS Mutants with Caveolin. To address the specificity of the interaction between caveolin and eNOS, we have explored the ability of caveolin antibodies to immunoprecipitate several deleted and truncated eNOS mutants recombinantly expressed in COS-7 cells. The cDNA constructs have previously been characterized (*6*, *25*); a schematic representation of the encoded proteins is shown in Figure 1A. Truncated isoforms lacking the N-terminal half (Δ1−511) or C-terminal half (Δ529−1205) of eNOS as well as isoforms deleted in the N-terminal half but containing the myristoylation site (Δ12−507) or both the palmitoylation and myristoylation sites (Δ85−507) have been used and compared with the WT-eNOS; immunoblots are presented in Figure 1B (upper panel). The interactions of these different truncated and deleted eNOS isoforms with caveolin-1 have been studied after lysis and solubilization in the CHAPS buffer, as previously described (*23*−*25*). We have also compared the pattern of coimmunoprecipitation when the detergent OG is substituted for CHAPS.

When immunoprecipitations were performed in the buffer containing CHAPS, caveolin antibodies immunoprecipitated WT-eNOS as well as the different truncated and deleted isoforms, with the notable exception of the truncated isoform lacking the N-terminal half of the enzyme (Δ1−511) (Figure 1B, middle panel). These data suggest that acylation (myristoylation) alone is sufficient for protein targeting to CHAPS-solubilized caveolin−protein complexes. We next repeated these experiments, solubilizing the eNOS−caveolin complexes with the detergent OG, with the expectation that this detergent might more efficiently disrupt protein−lipid interaction, as reported elsewhere (*27*−*29*). The effect of OG was dramatic: anti-caveolin-1 antibodies only precipitated the WT-eNOS and the truncated isoform lacking the C-terminal half of the enzyme (Δ529−1205) (Figure 1B, lower panel). The eNOS mutants containing the acylation motifs of the N-terminus but lacking large portions of the N-terminal half of eNOS were no longer coimmunoprecipitated by anti-caveolin antibodies in the presence of OG. These data suggest that specific sites for interaction of eNOS with caveolin are located within the N-terminal half of the enzyme.

eNOS Oligomerization and Caveolin Interaction. We next explored the relative roles of acylation and caveolin association in the process of eNOS targeting to caveolae. We

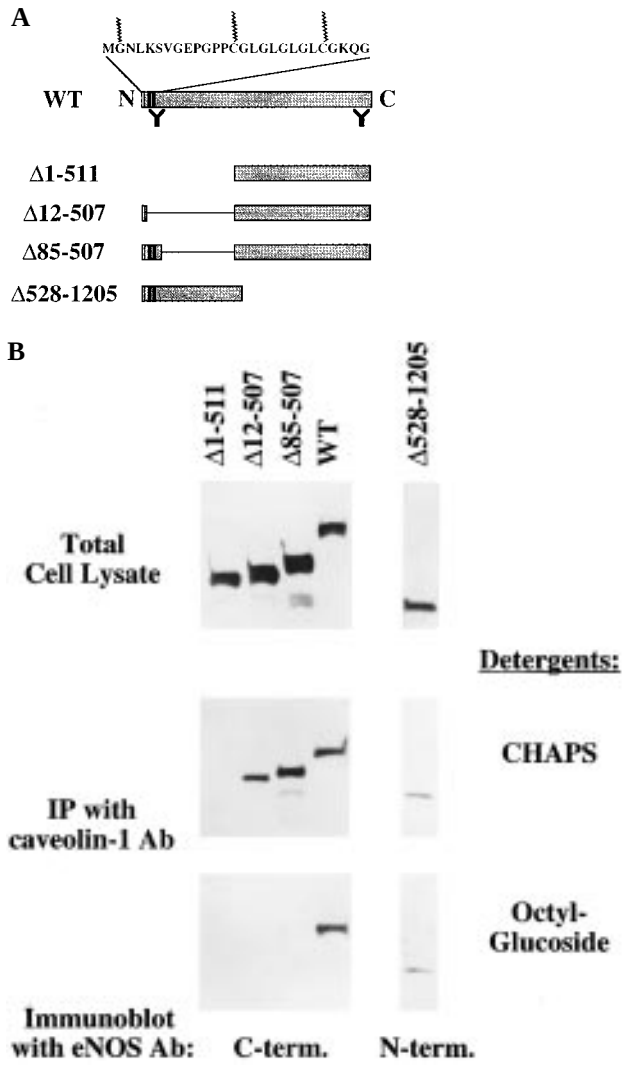

FIGURE 1: Characterization of the association between caveolin-1 and eNOS in COS-7 cells: behavior of truncated and deleted isoforms and the influence of detergents. (A) Map of the different deleted and truncated eNOS isoforms and localization of the different anti-eNOS antibodies used. Also shown above the schematic of the WT-eNOS are the N-terminal 30 aa, including the myristoylation site at Gly2 and the palmitoylation sites at Cys15 and Cys26. Note that the different truncated and deleted mutants are all catalytically inactive (Robinson & Michel, 1995). (B) The upper panel shows the immunoblots of WT-eNOS as well as of the different constructs transfected in COS-7 cells. The middle and lower panels show the eNOS immunoblots of caveolin-1 immunoprecipitations performed in the presence of CHAPS or OG, respectively; no difference was observed in the amounts of caveolin immunoprecipitated from CHAPS- and OG-solubilized transfected COS-7 cells (not shown). These experiments were repeated 2−3 times with equivalent results. A lower molecular weight band was variably seen in immunoblots of the Δ85−507 truncated eNOS mutant, possibly reflecting a degradation product of this internally deleted construct. Note that all the proteins were detected by a C-terminal anti-eNOS antibody, with the exception of the truncated isoform Δ528−1205, which was detected by an eNOS N-terminal antibody (the difference in the antibodies used in immunodetection may explain differences in the intensity of the bands observed).

performed cotransfection experiments, in which the myr$^-$ mutant [which is almost exclusively detected in the cytosol (*4*)] is coexpressed with the myristoylated Δ12−507 deleted isoform (which lacks the putative N-terminal caveolin binding region). Since heterodimeric complexes between the full-length and truncated eNOS can clearly form (*25*), we have explored whether the myristoyl group of the Δ12−

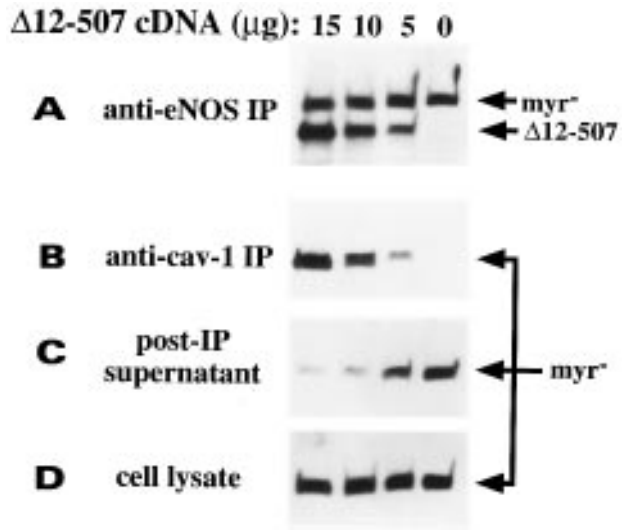

FIGURE 2: Rescue of myr⁻ mutant−caveolin-1 coimmunoprecipitation by coexpression of the truncated Δ12−507 isoform. COS-7 cells were transfected with an expression vector (5 μg per 100-mm plate) encoding the myr⁻ mutant, and the indicated amounts of Δ12−507 cDNA. Note that the amount of DNA in each transfection was kept constant by the addition of a β-galactosidase expression plasmid. Panel A shows the eNOS immunoblot (using a C-terminal antibody) of the eNOS immunoprecipitation (using an N-terminal antibody). Also shown are the eNOS immunoblots (using an N-terminal antibody) of immunoprecipitations performed from COS-7 cell lysates with anti-caveolin-1 antibodies (panel B) and from the supernatant of the caveolin immunoprecipitation (panel C). Panel D shows, for each condition, anti-eNOS immunoblotting (using an N-terminal antibody). These experiments were repeated 3 times with equivalent results.

507 isoform could promote the targeting of the myr⁻ mutant from its primary cytosolic location to caveolae and thus allows its association with caveolin. COS-7 cells were therefore transfected with the myr⁻ mutant construct plus increasing amounts of plasmids encoding the Δ12−507 isoform, and caveolin immunoprecipitations were performed in the presence of OG in order to exclude any interaction of the Δ12−507 isoform with caveolin (see Figure 1B).

When an antibody directed against the N-terminal end of eNOS was used to immunoprecipitate the myr⁻ mutant from COS-7 cell lysates, the Δ12−507 truncated protein (which is not recognized by this antibody) was detected in the immunoprecipitate (Figure 2A), indicating that the myr⁻ mutant and the deleted eNOS protein form heterodimers. Figure 2B shows that the myr⁻ mutant needs to be coexpressed with the Δ12−507 deletion eNOS mutant in order to be immunoprecipitated by caveolin-1 antibodies. With higher levels of expression of the Δ12−507 deleted isoform, the recovery of the myr⁻ mutant in the caveolin-1 immunoprecipitates was increased in parallel. We also analyzed the expression of myr⁻ mutant left behind in the supernatant of the immunoprecipitations. The amount of myr⁻ mutant (recovered by anti-eNOS immunoprecipitation) progressively decreased from 100% in the absence of the Δ12−507 deleted isoform to less than 10% in the presence of a 3-fold excess of the deleted isoform (Figure 2C), confirming that the Δ12−507 isoform, which undergoes myristoylation, is sufficient to promote caveolar targeting of the myr⁻ mutant. Figure 2D shows that the coexpression of increasing levels of the Δ12−507 truncated protein had no influence on the total amounts of myr⁻ mutant expressed.

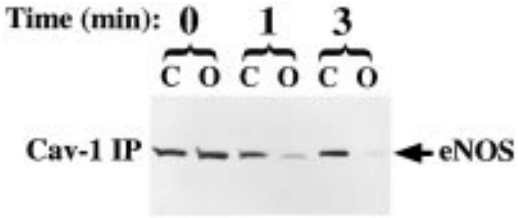

FIGURE 3: Inhibition of the association between caveolin-1 and eNOS by Ca^{2+} ionophore in endothelial cells. Shown are the eNOS immunoblots of anti-caveolin-1 immunoprecipitations from BAEC incubated in presence of 20 μM A23187 for 0, 1, and 3 min. Cells have been lysed, as described in the text, in CHAPS or OG buffers; in control experiments, the amounts of caveolin immunoprecipitated by caveolin-1 antibodies were not significantly different in the different detergent and time conditions (not shown). This experiment was repeated 3 times with equivalent results.

Perturbation of eNOS−Caveolin Interactions by Ca^{2+} Ionophore. We have recently shown that the eNOS−caveolin immunocomplex can be disrupted *in vitro* by binding of Ca^{2+}−calmodulin to eNOS (*24*). The next series of experiments investigated whether this interaction could also be altered in intact, cultured endothelial cells treated with the calcium ionophore A23187 (20 μM). By comparing the effects of CHAPS and OG to solubilize the caveolin complex, we have also attempted to further explore more subtle modifications in this model of dynamic regulation of eNOS. Figure 3 shows that after 1−3 min of incubation with the calcium ionophore A23187, CHAPS-solubilized eNOS can still be quantitatively immunoprecipitated from BAEC by caveolin-1 antibodies. However, when OG is used instead of CHAPS in the lysis and immunoprecipitation buffers, the recovery of eNOS in the caveolin-1 coimmunoprecipitation is decreased by 80% after 1 min, and this reduction persists for at least 10 min (data not shown).

Coexpression of Caveolin-1 with WT-eNOS or myr⁻ Mutant eNOS. The finding that eNOS may dissociate from caveolin following an increase in cytosolic Ca^{2+} concentration in intact endothelial cells suggests that the disruption of eNOS−caveolin interactions could constitute an early event preceding the translocation of eNOS from caveolae. Since the translocation of eNOS from caveolae likely alters the responsiveness of the enzyme, we designed experiments to explore whether eNOS association with caveolin can occur outside the caveolae environment. Thus, we have compared features of the predominantly membrane-associated WT enzyme with the cytosolic myr⁻ mutant (*4*) by performing cotransfection experiments in COS-7 cells using this eNOS mutant plus varying quantities of caveolin-1 cDNA. Caveolin is expressed in endothelial cells at a relatively high level (*30*); it seemed to us that a more tractable model to study the caveolin-dependent regulation of eNOS could exploit the presence of caveolae in COS-7 cells (*9*) and the low level of expression of endogenous caveolin in these cells, and we used the expression of recombinant caveolin in COS-7 cells to develop a cell system presenting different pools of caveolin. We thus explored the enzymatic activity of eNOS, as well as the ability of eNOS to be immunoprecipitated by caveolin antibodies, in cotransfection experiments using different levels of transfected caveolin-1 cDNA: 5, 10, and 15 μg of plasmid per 100 mm-plate of COS-7 cells; the levels of caveolin expressed (detected by

immunoblot analyses) were directly proportional to the cDNA amounts (not shown).

We showed that even without cotransfecting the caveolin cDNA, WT-eNOS can be nearly completely coimmunoprecipitated by its interaction with the endogenous caveolin-1 present in COS-7 cells (Figure 4A). The proportion of eNOS remaining in the supernatant fraction following immunoprecipitation with the caveolin antibody (Figure 4A, lower panel) confirmed that WT-eNOS, when coexpressed with the lowest quantity of caveolin-1 in these transfections, can be quantitatively immunoprecipitated by caveolin antibodies. In contrast, the myr$^-$ mutant required higher levels of caveolin-1 coexpression in COS-7 cells to be coimmunoprecipitated with caveolin (Figure 4A, upper panel). A quantitative coimmunoprecipitation was however observed at the highest levels of recombinant caveolin-1 expression used in our experiments (see Figure 4A, lower panel). We next analyzed the subcellular distribution of endogenous caveolin in COS-7 cells as well as the recombinant caveolin (following caveolin-1 cDNA transfection). Differential centrifugation (100000*g*, 1 h) revealed that caveolin-1, which was almost exclusively recovered in the particulate fraction from native COS-7 cells, was expressed in both supernatant and particulate subcellular fractions of transfected COS-7 cells (at the highest levels of recombinant caveolin expression) (Figure 4B). By contrast, most of the myr$^-$ mutant remained cytosolic at this high level of caveolin-1 coexpression (Figure 4B).

eNOS activity measurements were performed from parallel transfected COS-7 cell cultures. The coexpression of caveolin-1 and WT-eNOS led to a ~75% inhibition of the eNOS enzymatic activity measured in the absence of exogenous caveolin (Figure 4C). This inhibition was maximal even at the lowest level of caveolin-1 coexpression, since no additional inhibitory effect was observed when increasing amounts of caveolin-1 cDNA were transfected (Figure 4C). It should be noted that the experimental conditions used for the NOS enzyme activity assays differ markedly from the conditions used in these coimmunoprecipitation protocols, which may account for the apparent discordance between the substantial NOS inhibitory effect seen with exogenous caveolin expression in the face of our coimmunoprecipitation data showing a relatively low level of eNOS not associated with exogenous caveolin. Post-hoc caveolin−eNOS association (see below) may also lead to an overestimation of the fraction of eNOS complexed with caveolin in the resting cells.

The enzymatic activity of the myr$^-$ mutant was attenuated by coexpression of caveolin-1 in COS-7 cells only at higher levels of caveolin expression, but eventually reached the level of enzyme inhibition observed with WT-eNOS (Figure 4C). For both WT-eNOS and the myr$^-$ mutant, the inhibition of enzyme activity was completely reversed by addition of purified calmodulin to the enzyme assay (Figure 4C, hatched columns). We have previously observed that addition of a very large excess of exogenous calmodulin can increase eNOS activity over "basal" levels, presumably by attenuating the enzyme inhibition that is due to endogenous caveolin (*24*).

Coexpression of the palm$^-$ Mutant eNOS with Caveolin-1. The results obtained with the myr$^-$ mutant prompted us to analyze the influence of caveolin-1 on the activity of the palmitoylation-deficient eNOS mutant (palm$^-$). Although

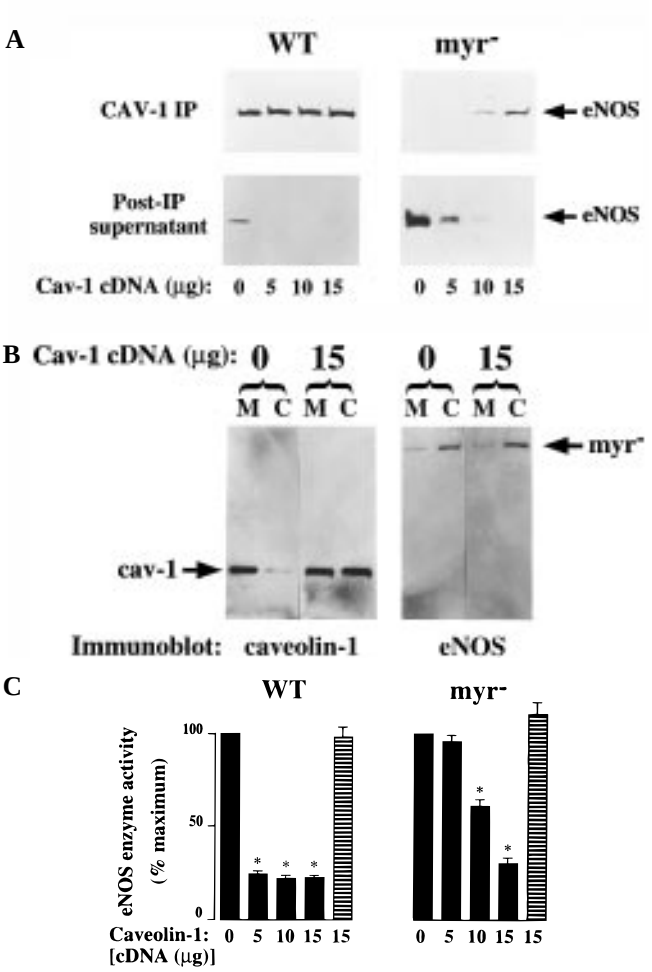

FIGURE 4: Influence of the levels of caveolin-1 expression in COS-7 cells (A) on the association of recombinant WT-eNOS and myr$^-$ mutant with caveolin, (B) on the subcellular distribution of caveolin and myr$^-$ mutant, and (C) on the enzymatic activity of WT-eNOS and myr$^-$ mutant. (A) Shown are the eNOS immunoblots of immunoprecipitations performed from transfected COS-7 cell lysates with anti-caveolin-1 antibodies (upper panel) and from the supernatant of the caveolin immunoprecipitation using anti-eNOS antibodies (lower panel). COS-7 cells were transfected with expression vectors (5 μg per 100-mm plate) encoding WT-eNOS or the myr$^-$ mutant, and increasing amounts of caveolin cDNA, as detailed in the text. Note that the amount of DNA in each transfection was kept constant by the addition of a β-galactosidase expression plasmid; caveolin immunoblots did not reveal any significant differences between WT-eNOS and myr$^-$ mutant cotransfection experiments (not shown). These experiments were repeated 3 times with equivalent results. Note that a large part of WT-eNOS can be immunoprecipitated by caveolin-1 antibodies without the need to coexpress recombinant caveolin-1, indicating a basal expression of caveolin in COS-7 cells. (B) Shown are the eNOS and caveolin immunoblots from the cytosolic (C) and membrane (M) fractions of COS-7 cells that have been transfected with the myr$^-$ mutant alone or with the myr$^-$ mutant and the highest level of caveolin DNA used in this study (15 μg per 100-mm plate); the conditions of transfection are the same as described above. This experiment was repeated twice with equivalent results. (C) Shown are the results of a [^{3}H]-L-arginine → [^{3}H]-L-citrulline NOS activity assay performed in cell lysates. These experiments were conducted in duplicate and are the means of four independent measurements. The hatched columns represent the NOS activity assayed in the presence of large excess of purified calmodulin (100 μM).

the intrinsic catalytic properties of the palm$^-$ eNOS mutant and the WT-enzyme have been shown to be identical (*31*), this mutant, although myristoylated (*19*), is not selectively targeted to caveolae, with a substantive fraction of the palm$^-$

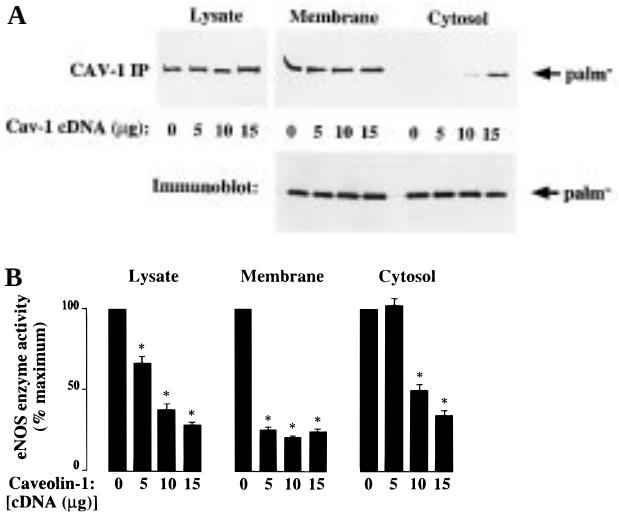

FIGURE 5: Influence of the level of caveolin-1 expression in COS-7 cells (A) on the association of the recombinant palm$^-$ mutant with caveolin in particulate and cytosolic fractions, and (B) on its enzymatic activity. (A) Shown are the eNOS immunoblots of immunoprecipitations performed from total cell lysates or from the cytosolic and particulate fractions, with anti-caveolin-1 antibodies (upper panel). COS-7 cells were transfected with expression vectors (5 μg per 100-mm plate) encoding the palm$^-$ mutant, and increasing amounts of caveolin cDNA, as detailed in the text. Note that the amount of DNA in each transfection was kept constant by the addition of a β-galactosidase expression plasmid. The anti-eNOS immunoblots, in the lower panel, show the distribution of the palm$^-$ mutant between the cytosolic and particulate fractions. This experiment was repeated 3 times with equivalent results. (B) Shown are the results of a [^{3}H]-L-arginine → [^{3}H]-L-citrulline NOS activity assay performed in total lysates and after subcellular fractionation; the conditions of transfection are the same as described above. These experiments were conducted in duplicate and are the means of three independent measurements.

expression still located in the soluble fraction of transfected COS-7 cells (*6*, *9*). We first examined the ability of caveolin-1 antibodies to immunoprecipitate the palm$^-$ mutant, in the presence or in the absence of recombinant caveolin-1 expression in COS-7 cells. The result of the immunoprecipitations from the CHAPS-solubilized COS-7 cell total lysates shows that the palm$^-$ mutant was nearly quantitatively associated with the endogenously expressed caveolin isoform (Figure 5A). A small but reproducible increase in the amount of immunoprecipitation was however observed with higher levels of caveolin expression. When COS-7 cell total lysates were submitted to a 100000*g* ultracentrifugation, and both particulate and cytosolic fractions were solubilized in the CHAPS buffer, the subsequent caveolin immunoprecipitations revealed distinct patterns. While the particulate palm$^-$ mutant was quantitatively immunoprecipitated by caveolin antibodies under all conditions, the cytosolic palm$^-$ mutant could be immunoprecipitated by caveolin-1 antibodies only at the highest levels of recombinant caveolin-1 expression (Figure 5A). Importantly, the distribution of the palm$^-$ between the particulate and cytosolic subcellular fractions was not altered by increasing caveolin expression (Figure 5A, lower panel). Together, these data suggest that a dynamic equilibrium exists between the particulate and cytosolic palm$^-$ mutants. The overexpression of recombinant caveolin in COS-7 cells does not appear to modify this equilibrium, which appears to be determined principally by the nature of eNOS acylation.

The enzymatic activity of the palm$^-$ mutant, measured in transfected COS-7 cell total lysates, was reduced in a dose-dependent fashion by the caveolin-1 coexpression (Figure 5B); as found for the WT and myr$^-$ eNOS (Figure 4C), the inhibition of the palm$^-$ mutant by caveolin was completely reversed by adding purified calmodulin to the enzyme activity assay (not shown). Following fractionation of transfected cells into particulate and soluble fractions by differential ultracentrifugation (100000*g*, 1 h), a striking shift in the pattern of enzyme inhibition was observed. The eNOS enzyme activity in the particulate fraction was reduced by more than 75% even at the lowest level of caveolin-1 cotransfection. By contrast, in the cytosolic fraction of the palm$^-$ mutant, there was no significant enzyme inhibition until higher caveolin-1 coexpression was achieved (Figure 5B). Thus, inhibition of the cytosolic fraction of the palm$^-$ mutant is not seen except under conditions where caveolin expression led to caveolin being present in the soluble fraction (see Figure 4B). This was confirmed in experiments in which the cytosolic fractions of palm$^-$ mutant and caveolin-1, individually obtained from separate cDNA transfections in COS-7 cells, were combined *in vitro* (not shown). A significant attenuation of eNOS enzyme activity was indeed seen when the cytosolic fractions of these two populations of transfected COS-7 cells were mixed *post-hoc* and assayed for NOS activity.

DISCUSSION

N-Myristoylation and thiopalmitoylation of eNOS are two covalent modifications required for the targeting of the enzyme to caveolae (*9*). In this report, we have documented the existence of a specific interaction between the scaffolding protein caveolin and eNOS, and we have shown that the dual acylation of eNOS, although favoring caveolar targeting, is not required for its interaction with caveolin. Moreover, our finding that caveolin−eNOS association may be disrupted in intact, cultured endothelial cells following agonist-induced increase in $[Ca^{2+}]_i$, combined with the observation that both proteins may be found associated outside the plasmalemmal caveolar environment, allows us to propose a model in which caveolin acts as a chaperone for eNOS.

These findings mostly derived from the exploitation of the differential effects of detergents, namely, CHAPS *vs* OG, for solubilizing the heteromeric caveolin complex. In our recent reports (*23*, *24*, *32*), we used CHAPS in our lysis and immunoprecipitation buffers since this detergent had been shown to preserve the oligomeric structure of eNOS (*25*) and to be particularly efficient to solubilize caveolin oligomeric complexes, possibly because of its structural similarity with cholesterol, one of the major lipid components of caveolae (*29*). However, OG has been shown to more efficiently solubilize Triton-insoluble domains than CHAPS (*27*) and, more specifically, to facilitate the solubilization of CHAPS-insoluble complexes such as the post-Golgi exocytic vesicles rich in GPI-linked proteins and caveolin (*28*, *29*). When applied to the characterization of the nature of interaction between caveolin and eNOS, the use of both detergents revealed distinct features (Figure 1). Indeed, when transfected COS-7 cells were lysed in presence of CHAPS, caveolin-1 antibodies could immunoprecipitate an internal deletion eNOS mutant comprised of only the 12 first N-terminal amino acids attached to the C-terminal half of

the enzyme: all that is required is that the myristoylation consensus sequence be retained in this deleted cDNA construct (see Figure 1A). Together with the observation that the dually acylated N-terminal half of eNOS could also coimmunoprecipitate with caveolin, it can be postulated that myristoylation alone can target eNOS to caveolin complexes independently of the rest of the sequence. However, the absence of association between caveolin and the C-terminal half of eNOS suggested that the caveolin interacts preferentially with the N-terminal half of the enzyme. In the presence of OG, only the association of caveolin with WT-eNOS or the N-terminal half of the enzyme was maintained, demonstrating that an intact eNOS N-terminal domain is required for stable interactions with caveolin. Taken together, these data indicate that, although acylation facilitates the interaction of eNOS with caveolin by targeting the enzyme to caveolae, a sequence within the eNOS N-terminal half accounts for the specificity and the stability of this interaction.

To confirm the respective roles of acylation and direct caveolin interaction for targeting eNOS to caveolae, we have coexpressed the myr$^-$ mutant with the C-terminal half of eNOS (Δ12−507), which is myristoylated but does not contain the N-terminal region potentially involved in the association with caveolin-1. We have previously reported that these recombinant proteins can form heterooligomers (*25*) and that the myr$^-$ mutant, which is neither myristoylated nor palmitoylated (*4*), is not targeted to caveolae (*9*). Here, we showed that the myr$^-$ mutant does not associate with endogenous caveolin in COS-7 cells, but can dose-dependently be recovered from the caveolin immunoprecipitation when coexpressed with the Δ12−507 deleted isoform (Figure 2). This indicates that, by forming a heteromeric complex, the myristoylated Δ12−507 deleted isoform can rescue the myr$^-$ mutant by promoting its targeting to caveolae, where the myr$^-$ mutant can then interact with caveolin through its intact N-terminal half. The use of OG as detergent in these experiments prevented the association of the Δ12−507 deleted isoform with caveolin, and we therefore infer that this truncated mutant serves primarily as a shuttle to target the full-length nonmyristoylated eNOS mutant to caveolae. Moreover, coexpression of the myr$^-$ mutant with the nonacylated truncated isoform Δ1−511 failed to induce detectable caveolin immunoprecipitation of the myr$^-$ mutant (not shown). Together, these results illustrate the distinct but complementary roles played by acylation and caveolin interaction in the posttranslational targeting and compartmentation of eNOS within caveolae.

The sequence analysis of the deleted and truncated isoforms used in these studies indicates that putative binding sites for caveolin are located between residues 85 and 528 of the bovine eNOS isoform; this is in agreement with the restriction of caveolin interaction to the eNOS oxygenase domain, recently reported by Ju et al. (*33*) using a yeast two-hybrid system approach. Our results allow us to exclude the sequence involved in the dual acylation of the enzyme, and delimit a region where the privileged targets for the regulatory interaction of caveolin are the heme domain, the calmodulin binding region, and the potential binding sites for L-arginine (*34*) and tetrahydrobiopterin (*35*). By blocking the access to these essential cofactors, caveolin could indeed maintain the enzyme in its inactivated state. Interestingly, Lisanti and co-workers (*21*, *22*) have recently identified, from phage display libraries, consensus peptide sequences rich in aromatic residues responsible for the specific interaction with caveolin. This putative consensus sequence exists within eNOS (bovine isoform: amino acids 350−358) and could therefore be directly involved in a protein−protein interaction with the caveolin scaffolding domain (*36*).

Another major finding derived from the differential effects of CHAPS *vs* OG in their ability to solubilize the caveolin heteromeric complex was the identification in intact endothelial cells of a Ca^{2+}-dependent process leading to the disruption of the caveolin/eNOS association. Indeed, when endothelial cells were treated with a calcium ionophore, the eNOS−caveolin coimmunoprecipitation was rapidly lost if the immunoprecipitation was performed in the presence of OG (Figure 3). In parallel coimmunoprecipitation experiments performed instead in the presence of CHAPS, we failed to document any change in eNOS−caveolin association. These discrepancies can be explained by the fact that CHAPS does not allow the discrimination between direct caveolin association and acylation-driven interaction of eNOS with caveolin complexes, the latter being abrogated by OG (see Figure 1). We have previously shown *in vitro* that Ca^{2+}−CaM promotes dissociation of the eNOS−caveolin immune complex (*24*) and that the caveolin scaffolding domain functions as a competitive inhibitor of the allosteric activation of eNOS by Ca^{2+}−CaM (*37*). The results obtained here, in an intact cell system, confirm that the agonist-induced Ca^{2+}/CaM-dependent dissociation of eNOS from its scaffold caveolin is the physiological trigger responsible for the activation of the enzyme, and that, consequently, the reassociation of the two proteins ends NO production. Furthermore, since eNOS undergoes depalmitoylation (*19*) and subcellular translocation following agonist stimulation (*38*), we can postulate that caveolin may remain associated (or reassociate) with the enzyme to serve as an inhibitory chaperone of eNOS following its depalmitoylation and consequent dislocation from plasmalemmal caveolae. This hypothesis is supported by the present studies which establish that eNOS does not have to be located in caveolae to interact with caveolin. We have indeed shown that the cytosol-restricted myr$^-$ mutant and the soluble fraction of the palm$^-$ mutant may both interact with caveolin, leading to a marked (Ca^{2+}/CaM-reversible) inhibition of their enzyme activity (Figures 4 and 5). The presence of caveolin in the soluble compartments of endothelial cells has been previously reported (*39*) and may be generalized since it has been shown that caveolae assemble in the cytosol during transport to the plasma membrane (*40*) and constitutively cycle, via the cytosol, between plasma membrane and the Golgi (*41*). Based on these data, we therefore propose that the "soluble fraction" of the cell, possibly subplasmalemmal vesicles or the cytoplasmic face of the trans-Golgi network, provides the locale wherein depalmitoylated eNOS may reassociate with caveolin following agonist-induced translocation from caveolae.

In conclusion, our data demonstrate the existence of a direct, regulatory -eNOS−caveolin interaction that appears to be independent of the state of eNOS acylation, indicating that agonist-promoted depalmitoylation of eNOS is unlikely to relieve the tonic inhibition of the enzyme activity. We therefore postulate the existence of a dynamic equilibrium

between inactive caveolin-associated eNOS and activated CaM-bound eNOS, with agonist-induced calcium transients being responsible for the transition from one to the other state. In this model, the reversible palmitoylation of eNOS serves principally as a determinant of the enzyme's subcellular targeting, and agonist-evoked eNOS depalmitoylation appears unlikely to modulate the inhibitory association between eNOS and caveolin: this role is clearly subserved by the binding of Ca^{2+}−CaM to the enzyme.

REFERENCES

1. Marletta, M. (1994) *Cell 78*, 927−930.
2. Nathan, C., and Xie, Q.-W. (1994) *J. Biol. Chem. 269*, 13725−13728.
3. Sase, K., and Michel, T. (1996) *Trends Cardiovasc. Med. 7*, 28−37.
4. Busconi, L., and Michel, T. (1993) *J. Biol. Chem. 268*, 8410−8413.
5. Liu, J., and Sessa, W. C. (1994) *J. Biol. Chem. 269*, 11691−11694.
6. Robinson, L. J., and Michel, T. (1995) *Proc. Natl. Acad. Sci. USA 92*, 11776−11780.
7. Boutin, A. (1997) *Cell. Signalling 9*, 15−35.
8. Miligan, G., Parenti, M., and Magee, A. I. (1995) *Trends Biochem. Sci. 20*, 101−107.
9. Shaul, P. W., Smart, E. J., Robinson, L. J., German, Z., Yuhanna, I. S., Ying, Y., Anderson, R. G. W., and Michel, T. (1996) *J. Biol. Chem. 271*, 6518−6522.
10. Lisanti, M. P., Scherer, P. E., Tang, Z., and Sargiacomo, M. (1994) *Trends Cell. Biol. 4*, 231−235.
11. Parton, R. G. (1996) *Curr. Opin. Cell Biol. 8*, 542−548.
12. Liu, J., Oh, P., Horner, T., Rogers, R. A., and Schnitzer, J. E. (1997) *J. Biol. Chem. 272*, 7211−7222.
13. Shenoy-Scarcia, A. M., Dietzen, D. J., Kwong, J., Link, D. C., and Lublin, D. M. (1994) *J. Cell Biol. 126*, 353−363.
14. Wedegaertner, P. B., Wilson, P. T., and Bourne, H. R. (1995) *J. Biol. Chem. 270*, 503−506.
15. Liu, L., Dudler, T., and Gelb, M. H. (1996) *J. Biol. Chem. 271*, 23269−23276.
16. Dietzen, D. J., Hastings, W. R., and Lublin, D. M. (1995) *J. Biol. Chem. 270*, 6838−6842.
17. Monier, S., Dietzen, D. J., Hastings, W. R., Lublin, D. M., and Kurzchalia, T. V. (1996) *FEBS Lett. 388*, 143−149.
18. Kübler, E., Dohlman, H. G., and Lisanti, M. P. (1996) *J. Biol. Chem. 271*, 32975−32980.
19. Robinson, L. J., Busconi, L., and Michel, T. (1995) *J. Biol. Chem. 270*, 995−998.
20. Song, K. S., Li, S., Okamoto, T., Quilliam, L. A., Sargiacomo, M., and Lisanti, M. P. (1996) *J. Biol. Chem. 271*, 9690−9697.
21. Li, S., Couet, J., and Lisanti, M. P. (1996) *J. Biol. Chem. 271*, 29182−29190.
22. Couet, J., Li, S., Okamoto, T., Ikezu, T., and Lisanti, M. P. (1997) *J. Biol. Chem. 272*, 6525−6533.
23. Feron, O., Belhassen, L., Kobzik, L., Smith, T. W., Kelly, R. A., and Michel, T. (1996) *J. Biol. Chem. 271*, 22810−22814.
24. Michel, J. B., Feron, O., Sacks, D., and Michel, T. (1997) *J. Biol. Chem. 272*, 15583−15587.
25. Lee, C. M., Robinson, L. J., and Michel, T. (1995) *J. Biol. Chem. 270*, 27403−27406.
26. Bredt, D. S., and Snyder, S. H. (1990) *Proc. Natl. Acad. Sci. U.S.A. 87*, 682−685.
27. Hooper, N. G., and Turner, A. J. (1988) *Biochem. J. 250*, 865−869.
28. Kurzchalia, T. V., Dupree, P., Parton, R. G., Kellner, R., Virta, H., Lehnert, M., and Simons, K. (1992) *J. Cell Biol. 118*, 1003−1014.
29. Sargiacomo, M., Sudol, M., Tang, Z., and Lisanti, M. P. (1993) *J. Cell Biol. 122*, 789−807.
30. Schnitzer, J., Siflinger-Birnboim, A., Del Vecchio, P. J., and Malik, A. B. (1994) *Biochem. Biophys. Res. Commun. 199*, 11−19.
31. Liu, J., Garcia-Gardena, G., and Sessa, W. C. (1996) *Biochemistry 35*, 13277−13281.
32. Feron, O., Smith, T. W., Michel, T., and Kelly, R. A. (1997) *J. Biol. Chem. 272*, 17744−17748.
33. Ju, H., Zou, R., Venema, V. J., and Venema, R. C. (1997) *J. Biol. Chem. 272*, 18522−18525.
34. Chen, P.-F., Tsai, A.-L., Berka, V., and Wu, K. K. (1997) *J. Biol. Chem. 272*, 6114−6118.
35. Rodriguez-Crespo, I., Gerber, N. C., and Ortiz de Montellano, P. R. (1996) *J. Biol. Chem. 271*, 11462−11467.
36. Garcia-Gardena, G., Martasek, P., Siler Masters, B. S., Skidd, P. M., Couet, J., Li, S., Lisanti, M. P., and Sessa, W. C. (1997) *J. Biol. Chem. 272*, 25437−25440.
37. Michel, J. B., Feron, O., Sase, K., Prabhakar, P., and Michel, T. (1997) *J. Biol. Chem. 272*, 25907−25912.
38. Michel, T., Li, G. K., and Busconi, L. (1993) *Proc. Natl. Acad. Sci. U.S.A. 90*, 6252−6256.
39. Venema, V. J., Zou, R., Ju, H., Marrero, M. B., and Venema, R. C. (1997) *Biochem. Biophys. Res. Commun. 236*, 155−161.
40. Monier, S., Parton, R. G., Vogel, F., Behlke, J., Henske, A., and Kurzchalia, T.V. (1995) *Mol. Biol. Cell 6*, 911−927.
41. Conrad, P., Smart, E., Ying, Y.-S., Anderson, R. G. W., and Bloom, G. S. (1995) *J. Cell Biol. 131*, 1421−1433.

BI972307P